Cell

O-GlcNAc Transferase Catalyzes Site-Specific Proteolysis of HCF-1

Francesca Capotosti,[1] Sophie Guernier,[1] Fabienne Lammers,[1] Patrice Waridel,[2] Yong Cai,[3,5] Jingji Jin,[3,5] Joan W. Conaway,[3,4] Ronald C. Conaway,[3,4] and Winship Herr[1,*]

[1]Center for Integrative Genomics, University of Lausanne, Génopode, 1015 Lausanne, Switzerland

[2]Protein Analysis Facility, Center for Integrative Genomics, Faculty of Biology and Medicine, University of Lausanne, 1015 Lausanne, Switzerland

[3]Stowers Institute for Medical Research, Kansas City, MO 64110, USA

[4]Department of Biochemistry and Molecular Biology, University of Kansas Medical Center, Kansas City, KS 66160, USA

[5]Present address: College of Life Sciences, Jilin University, 2699 Qianjin Street, Changchun, Jilin Province 130012, China

*Correspondence: winship.herr@unil.ch

DOI 10.1016/j.cell.2010.12.030

SUMMARY

The human epigenetic cell-cycle regulator HCF-1 undergoes an unusual proteolytic maturation process resulting in stably associated HCF-1_N and HCF-1_C subunits that regulate different aspects of the cell cycle. Proteolysis occurs at six centrally located HCF-1_{PRO}-repeat sequences and is important for activation of HCF-1_C-subunit functions in M phase progression. We show here that the HCF-1_{PRO} repeat is recognized by *O*-linked β-*N*-acetylglucosamine transferase (OGT), which both *O*-GlcNAcylates the HCF-1_N subunit and directly cleaves the HCF-1_{PRO} repeat. Replacement of the HCF-1_{PRO} repeats by a heterologous proteolytic cleavage signal promotes HCF-1 proteolysis but fails to activate HCF-1_C-subunit M phase functions. These results reveal an unexpected role of OGT in HCF-1 proteolytic maturation and an unforeseen nexus between OGT-directed *O*-GlcNAcylation and proteolytic maturation in HCF-1 cell-cycle regulation.

INTRODUCTION

The informational complexity of organisms can be greatly enhanced by the posttranslational modification of proteins. Modifications that involve the addition of a chemical group, such as phosphorylation, acetylation, methylation, glycosylation, and ubiquitination, are generally reversible, whereas modification by proteolytic processing is considered irreversible. The variety of modification forms and their regulatory outcomes provides diverse strategies for the control of protein function.

Among modifications involving the addition of a chemical group, glycosylation is the most abundant (Nalivaeva and Turner, 2001) and, of the different types of glycosylation, the monoaddition of *O*-linked β-*N*-acetylglucosamine (*O*-GlcNAc) moieties on serine and threonine residues is the most important to regulate the function of metazoan cytosolic and nuclear proteins (Torres and Hart, 1984; Wells and Hart, 2003). The broad presence of *O*-GlcNAc-modified proteins involved in many fundamental cellular processes, including cell morphogenesis, cell signaling, apoptosis, and transcription, suggests important physiological roles for *O*-GlcNAcylation (Lazarus et al., 2006). *O*-GlcNAcylation exhibits similarities to phosphorylation, such as common target residues (i.e., serines and threonines), proteins, and dynamic nature (Hart et al., 2007; Wells and Hart, 2003; Wells et al., 2001), but differs in that *O*-GlcNAcylation is achieved by a single cellular enzyme: *O*-GlcNAc transferase (OGT) (Haltiwanger et al., 1992).

OGT is a ubiquitously expressed and conserved enzyme that uses the donor substrate UDP-GlcNAc for glycosylation. It is composed of two important regions: an N-terminal 13.5 tetratricopeptide-repeat (TPR) superhelical structure (Jinek et al., 2004), involved in substrate recognition (Lubas and Hanover, 2000), and a C-terminal catalytic domain (Kreppel and Hart, 1999). The catalytic domain contains the UDP-GlcNAc binding site but the precise mechanism of *O*-GlcNAc transfer to substrates is not known (Clarke et al., 2008; Martinez-Fleites et al., 2008). OGT forms stable associations with numerous proteins, such as the histone acetyltransferase MOF (Cai et al., 2010), the protein phosphatase PP1 (Wells et al., 2004), the transcriptional corepressor Sin3A (Yang et al., 2002), and the cell-cycle regulator HCF-1 (Wysocka et al., 2003; Mazars et al., 2010), the subject of this study.

HCF-1 is a transcriptional coregulator conserved among animal species that was first discovered as a host-cell factor for human herpes simplex virus infection (Kristie et al., 2010; Wysocka and Herr, 2003). In vertebrates, HCF-1 undergoes an unusual process of proteolytic maturation. It is synthesized as a large precursor protein that is subsequently cleaved at a series of six centrally located 26 amino acid repeats called HCF-1_{PRO} (PRO for proteolysis) repeats. The resulting heterogeneous collection of N- (HCF-1_N) and C- (HCF-1_C) terminal subunits remains noncovalently associated (Kristie et al., 1995; Wilson et al., 1993, 1995). An important cellular function of human HCF-1 is the regulation of the cell cycle: the HCF-1_N subunit promotes passage through the G1 phase (Goto et al., 1997; Julien and Herr, 2003; Tyagi and Herr, 2009) and the HCF-1_C

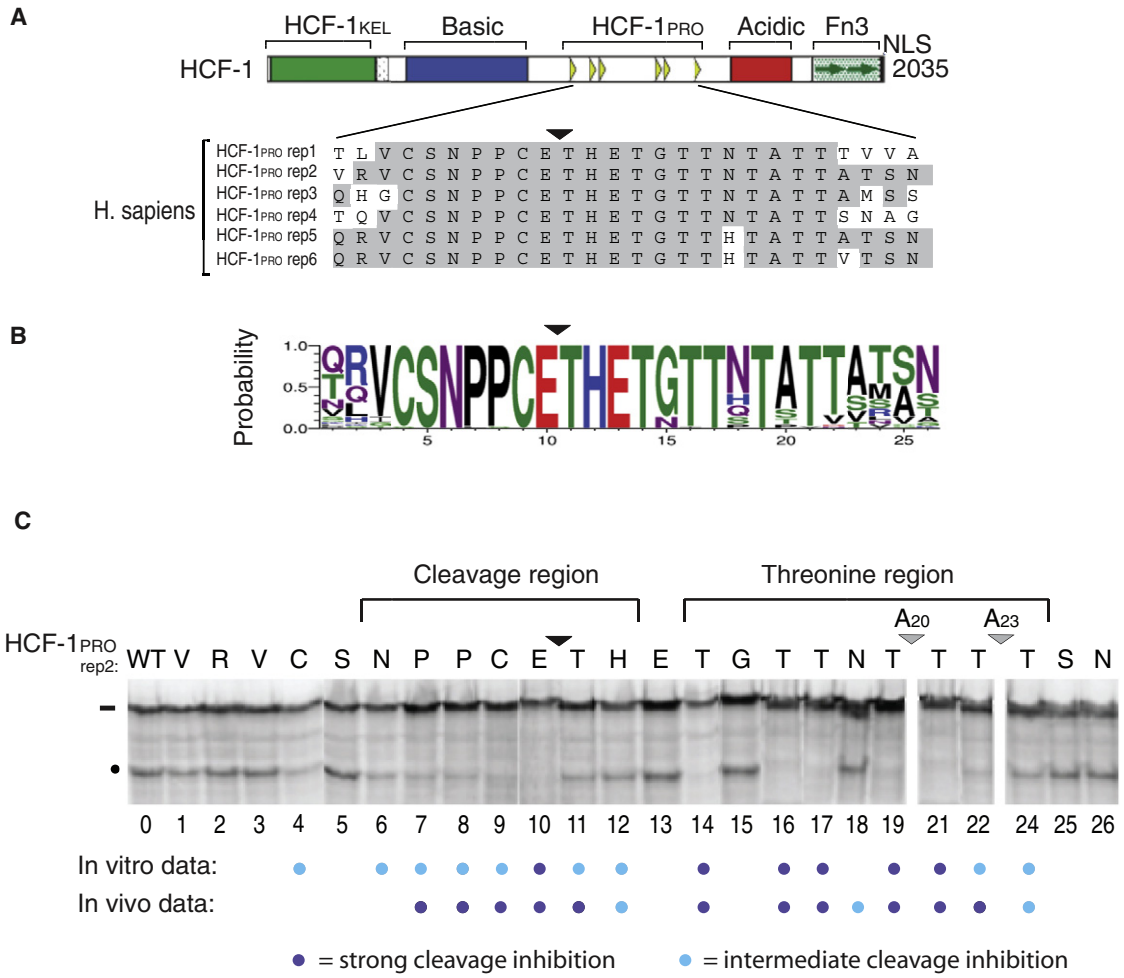

Figure 1. Sequence and In Vitro Mutational Analysis of HCF-1$_{PRO}$ Repeats

(A) Schematic representation of the human HCF-1 protein and sequence alignment of the six human HCF-1$_{PRO}$ repeats. The black arrowhead indicates the cleavage site.

(B) HCF-1$_{PRO}$-repeat sequence conservation. WebLogo (Crooks et al., 2004) was obtained by the alignment of all HCF-1$_{PRO}$ repeats from six different species: human, mouse, *Xenopus tropicalis*, *X. laevis*, *Fugu rubripes*, and *Danio rerio*.

(C) In vitro alanine-scan mutagenesis. The wild-type HCF-1$_{PROrep2}$ precursor (lane 0) as well as individual HCF-1$_{PROrep2}$ alanine mutants (lanes 1–19, 21, 22, and 24–26) were incubated with HeLa nuclear extract. The gray arrowheads indicate the positions of the two HCF-1$_{PROrep2}$ alanines that were not mutated. The precursor (–) and the visible N-terminal cleavage product (●) are indicated. Colored dots indicate mutations with strong (blue) or intermediate (cyan) effects on either in vitro or in vivo (Wilson et al., 1995) cleavage.

subunit ensures proper mitosis and cytokinesis in M phase (Julien and Herr, 2003, 2004). Interestingly, HCF-1 proteolytic maturation is necessary to activate human HCF-1$_C$-subunit function in M phase (Julien and Herr, 2003).

Curiously, the mechanism of HCF-1 proteolytic maturation has diverged in evolution. Whereas HCF-1$_{PRO}$-repeat-dependent HCF-1 maturation is apparently shared by, and restricted to, all vertebrate species, in some invertebrate species (e.g., *Drosophila*) HCF-1 homologs also undergo proteolytic maturation but by a different mechanism involving the protease Taspase1 (Capotosti et al., 2007). In vertebrates, Taspase1 is responsible for proteolytic maturation of the mixed-lineage leukemia (MLL) histone methyltransferase protein (Hsieh et al., 2003) but not of HCF-1 (Capotosti et al., 2007). How HCF-1$_{PRO}$-repeat-dependent proteolytic maturation is achieved remains to be clarified, as evidence supporting both autocatalytic (Vogel and Kristie, 2000) and nonautocatalytic (Capotosti et al., 2007) mechanisms has been reported.

We demonstrate here a connection between HCF-1$_{PRO}$-repeat-induced HCF-1 proteolytic maturation and OGT, providing an unexpected link between reversible and irreversible posttranslational modification pathways to control protein function.

RESULTS

The HCF-1$_{PRO}$ Repeat Represents an Elaborate Cleavage Signal

Figure 1A shows the close similarity among the six human HCF-1$_{PRO}$ repeats and the site of proteolytic cleavage, a glutamic acid at position 10 (E10) (arrowhead; Kristie et al., 1995; Wilson

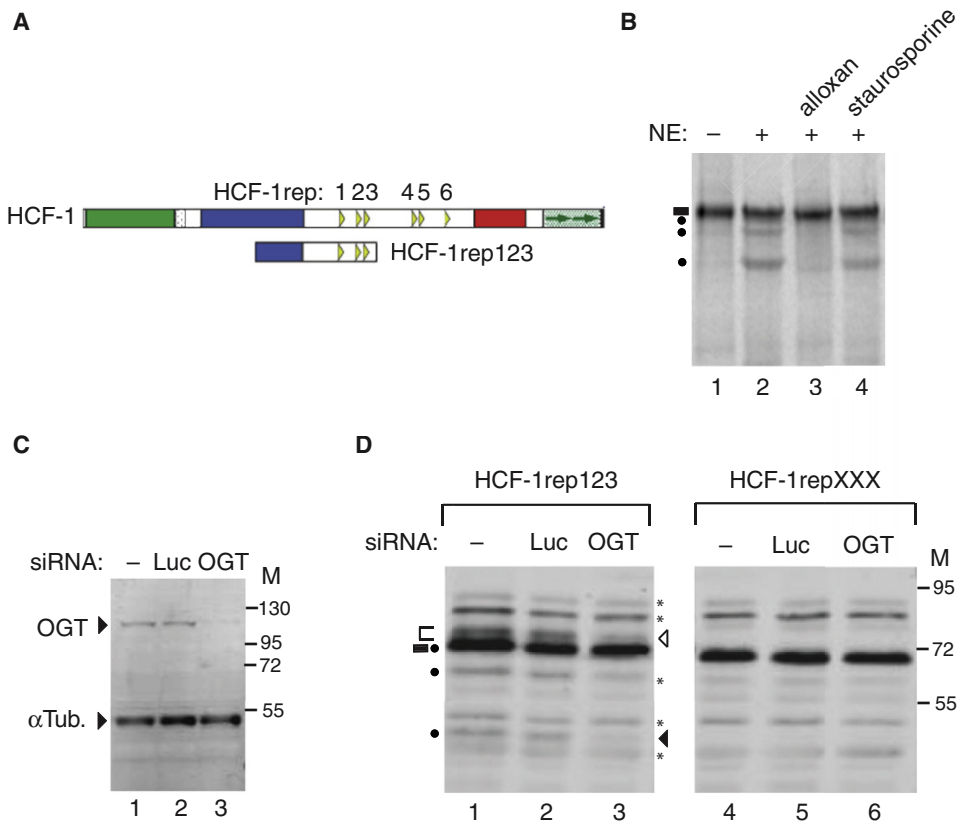

Figure 2. *O*-GlcNAcylation Is Important for HCF-1$_{PRO}$-Repeat Cleavage

(A) Schematic representation of full-length HCF-1 and HCF-1rep123.

(B) Inhibition of HCF-1$_{PRO}$-repeat cleavage. HCF-1rep123 synthesized in RRL was incubated with buffer (lane 1), HeLa nuclear extract (NE; lane 2), or NE pretreated with alloxan (lane 3) or staurosporine (lane 4).

(C) OGT depletion by siRNA. 293 cells were either mock treated (lane 1) or treated with luciferase- (Luc; lane 2) or OGT- (lane 3) specific siRNAs. OGT and α-tubulin (αTub.) levels were visualized by immunoblot.

(D) Effect of OGT depletion on HCF-1$_{PRO}$-repeat cleavage. Cells treated as in (C) were transiently transfected with the HCF-rep123 (lanes 1–3) and HCF-1repXXX (lanes 4–6) expression constructs. Precursor cleavage was analyzed by α-HA tag immunoblot. The bracket indicates the *O*-GlcNAc-modified HCF-1rep123 precursor. Empty and filled arrowheads indicate the *O*-GlcNAc-modified HCF-1rep123 precursor and HCF-1$_{PRO}$-repeat 1 cleavage product, respectively. Asterisks indicate nonspecific bands.

In (B) and (D), precursor proteins (–) and cleavage products (●) are indicated.

et al., 1993, 1995). A sequence logo generated from a multiple vertebrate species alignment highlights the extensive conservation of the HCF-1$_{PRO}$ repeats (Figure 1B).

For a protease recognition sequence, the HCF-1$_{PRO}$ repeat is large. Indeed, in vivo assay of a complete set of HCF-1$_{PRO}$-repeat 2 alanine-scan mutants revealed an 18 amino acid core required for full cleavage activity (Wilson et al., 1995). Using a previously described human HeLa cell extract assay (Capotosti et al., 2007), we tested cleavage of the same set of alanine-scan mutants in vitro, as shown in Figure 1C. The effect of the alanine substitutions was very similar to what was previously observed in vivo (Figure 1C), indicating that the in vitro assay faithfully reflects normal HCF-1 proteolytic maturation. The mutational analysis revealed a C-terminal HCF-1$_{PRO}$-repeat region with a number of conserved and functionally important threonine residues. We refer to this region as the "threonine region" and the sequences surrounding the cleavage site as the "cleavage region" (see Figure 1C).

A Role for OGT in HCF-1$_{PRO}$-Repeat Proteolysis In Vitro and In Vivo

Three observations led us to ask whether protein modification might be important for HCF-1$_{PRO}$-repeat cleavage: (1) the resistance of the HeLa cell proteolytic activity to fractionation, suggesting multiple components (F.C. and W.H., unpublished results); (2) a retarded electrophoretic mobility of the uncleaved HCF-1$_{PRO}$-repeat precursor after in vitro cleavage reaction (Capotosti et al., 2007), a property often indicative of posttranslational modification; and (3) the critical threonine region given that threonines can be sites for phosphorylation and *O*-GlcNAcylation. We therefore tested whether a general inhibitor of phosphorylation (staurosporine) or of *O*-GlcNAcylation (alloxan) affects processing in vitro of the HCF-1-derived precursor called HCF-1rep123 (Figure 2A). As shown in Figure 2B, alloxan, but not staurosporine, reduced HCF-1rep123 cleavage (compare lanes 3 and 4 with lane 2), suggesting a relationship between *O*-GlcNAcylation and HCF-1$_{PRO}$-repeat

cleavage and a possible role of OGT in HCF-1 proteolytic maturation.

To test this hypothesis, we asked whether depletion of OGT in vivo affects HCF-1rep123 processing. OGT can be significantly depleted after 48 hr of human 293 cell treatment with an OGT-specific (lane 3) but not an irrelevant (lane 2) siRNA duplex (Figure 2C). We assayed the effect of OGT depletion on cleavage of the wild-type HCF-1rep123 precursor and an HCF-1repXXX mutant with alanine-substituted E10 cleavage-site residues (E10A), synthesized during the last 24 hr of 48 hr siRNA treatment. HCF-1repXXX was not affected by OGT depletion (Figure 2D, lanes 4–6). In contrast, with HCF-1rep123, OGT depletion caused a specific (compare lanes 1–3) reduction of the HCF-1_{PRO}-repeat 1 cleavage product (filled arrowhead) and of a slower migrating—possibly modified—form of the precursor (open arrowhead). (Note that the products of HCF-1_{PRO}-repeat 2 and 3 cleavage are obscured by other species in this experiment.) Together, these results suggest a role for OGT and possibly *O*-GlcNAcylation in proteolytic processing of HCF-1.

The HCF-1rep123 Precursor Is *O*-GlcNAcylated in an HCF-1_{PRO}-Repeat-Dependent Manner

To test for a link between *O*-GlcNAcylation and proteolysis, we assayed glycosylation of HCF-1rep123 and HCF-1repXXX, together with the HCF-1_{PRO}-repeat 1-containing HCF-1rep1XX protein, in vivo. After synthesis in 293 cells, α-HA tag immunopurified recombinant proteins (Figure 3Aa) were probed for *O*-GlcNAcylation by immunoblot (Figure 3Ab). Consistent with HCF-1_{PRO}-repeat-dependent *O*-GlcNAcylation, the HCF-1rep123 and HCF-1rep1XX, but not HCF-1repXXX, precursors and cleavage products were readily recognized by the α-*O*-GlcNAc antibody (Figure 3Ab; lanes 1–3). The slower migration of the precursor observed here and in Figure 2D (see brackets) probably results from the *O*-GlcNAcylation as opposed to phosphorylation, as it was insensitive to phosphatase treatment (see Figure S1 available online). The HCF-1_{PRO}-repeat dependence of HCF-1rep123 *O*-GlcNAcylation was unexpected because we had hypothesized that glycosylation might activate HCF-1rep123 proteolysis, not that the HCF-1_{PRO} repeat might activate HCF-1rep123 glycosylation.

HCF-1_{PRO} Repeats Can Induce Multiple *O*-GlcNAc Modifications in the HCF-1_N Subunit

HCF-1 is *O*-GlcNAcylated (Wilson et al., 1993; Wysocka et al., 2003) at multiple sites (Mazars et al., 2010; Wang et al., 2010). Here we mapped *O*-GlcNAcylation sites in purified HCF-1rep123 and HCF-1repXXX precursors after in vivo synthesis. The HCF-1rep123 material (Figure 3B, lane 1) produced a doublet of faster- (a) and slower- (a′) migrating forms upon silver staining. In contrast, with HCF-1repXXX, the faster-migrating form (b) predominated (lane 2). These three polypeptides were individually analyzed by tandem mass spectrometry, and glycosylated and nonglycosylated peptides were identified and quantified (see Table S1). Figure 3C shows the results for one peptide (HCF-1 residues 724–770). This peptide from samples a and b was predominantly unmodified, whereas from sample a′ it was predominantly *O*-GlcNAcylated, consistent with HCF-1_{PRO}-repeat-dependent HCF-1 *O*-GlcNAcylation.

Figure 3D shows the results of our HCF-1rep123 *O*-GlcNAc modification mapping, together with sites mapped by Wang et al. (2010) within this region. Interestingly, the mapped sites exclude the HCF-1_{PRO}-repeats but include extensive N-terminal *O*-GlcNAc modifications. Thus, counter to our aforementioned rationale, the HCF-1_{PRO}-repeat threonine region is apparently not *O*-GlcNAc modified.

To obtain a global appreciation of HCF-1 *O*-GlcNAcylation, we analyzed *O*-GlcNAcylation of endogenous HCF-1, as shown in Figure 3E. Immunopurified endogenous HCF-1 was subjected to immunoblot analysis with antibodies specific to either the HCF-1_C or HCF-1_N subunit, or *O*-GlcNAc (lanes 1–3). The resulting *O*-GlcNAc staining pattern matches the HCF-1_N but not the HCF-1_C (lane 4)-subunit profile, suggesting that HCF-1 *O*-GlcNAcylation is largely limited to the HCF-1_N subunit (see also Mazars et al., 2010; Wang et al., 2010).

OGT Recognizes the HCF-1_{PRO} Repeat

The dependence of HCF-1 *O*-GlcNAcylation on active HCF-1_{PRO} repeats led us to ask whether the HCF-1_{PRO} repeat also promotes OGT binding to HCF-1. Analysis of the HCF-1rep123 immunoprecipitates from Figure 3A (see also Figure 4Aa) showed that OGT—present in the original extracts (Figure 4Ab)—was present in the HCF-1rep123 but not mock samples (Figure 4Ac, compare lanes 1 and 4). Indeed, OGT bound even better to the HCF-1rep1XX and HCF-1repXXX precursors carrying the E10A cleavage-site mutation (lanes 2 and 3). Thus, curiously, although inhibiting HCF-1_{PRO}-repeat cleavage and HCF-1rep123 glycosylation, the E10A mutation enhances OGT association with the HCF-1_{PRO}-repeat precursor.

These results led us to ask whether OGT association with HCF-1 can be mediated by the HCF-1_{PRO} repeat. For this, we tested OGT association with full-length HCF-1 and the four HCF-1 mutants illustrated in Figure 4B: (1) HCF-1_{PROMUT} carrying the E10A cleavage-site mutation in all six HCF-1_{PRO} repeats (the HCF-1nc mutant of Vogel and Kristie, 2006); (2) HCF-$1_{\Delta PRO}$, lacking the HCF-1_{PRO}-repeat region (Wilson et al., 1995), and (3) HCF-$1_{\Delta PROrep2}$ and (4) HCF-$1_{\Delta PROrep2E10A}$ carrying a single wild-type or mutated HCF-1_{PRO} repeat 2. Figure 4C shows the (1) levels of wild-type and mutant HCF-1 synthesis after transient expression (Figure 4Ca), (2) levels of endogenous OGT (Figure 4Cb), and (3) levels of OGT coprecipitated with the various HCF-1 proteins (Figure 4Cc). As with the HCF-1rep123 proteins, OGT was recovered with full-length HCF-1 and significantly better with HCF-1_{PROMUT} (lanes 2 and 3). Furthermore, the E10A HCF-$1_{\Delta PROrep2E10A}$ mutant bound OGT better than its wild-type HCF-$1_{\Delta PROrep2}$ counterpart (lanes 5 and 6). In contrast, there was no evident OGT association in the absence of an HCF-1_{PRO} repeat (see HCF-$1_{\Delta PRO}$; lane 4). These results indicate that the HCF-1_{PRO}-repeat sequence itself is the target for OGT binding and that the E10A mutation improves binding.

Threonine-Region Mutations Disrupt OGT Association with HCF-1_{PRO} Repeat 2

The E10A HCF-1_{PRO}-repeat substitution lies within the HCF-1_{PRO}-repeat cleavage region. To test the effect of mutations in the threonine region, we assayed endogenous OGT association with wild-type or mutated HCF-1_{PRO} repeats (repeat 2)

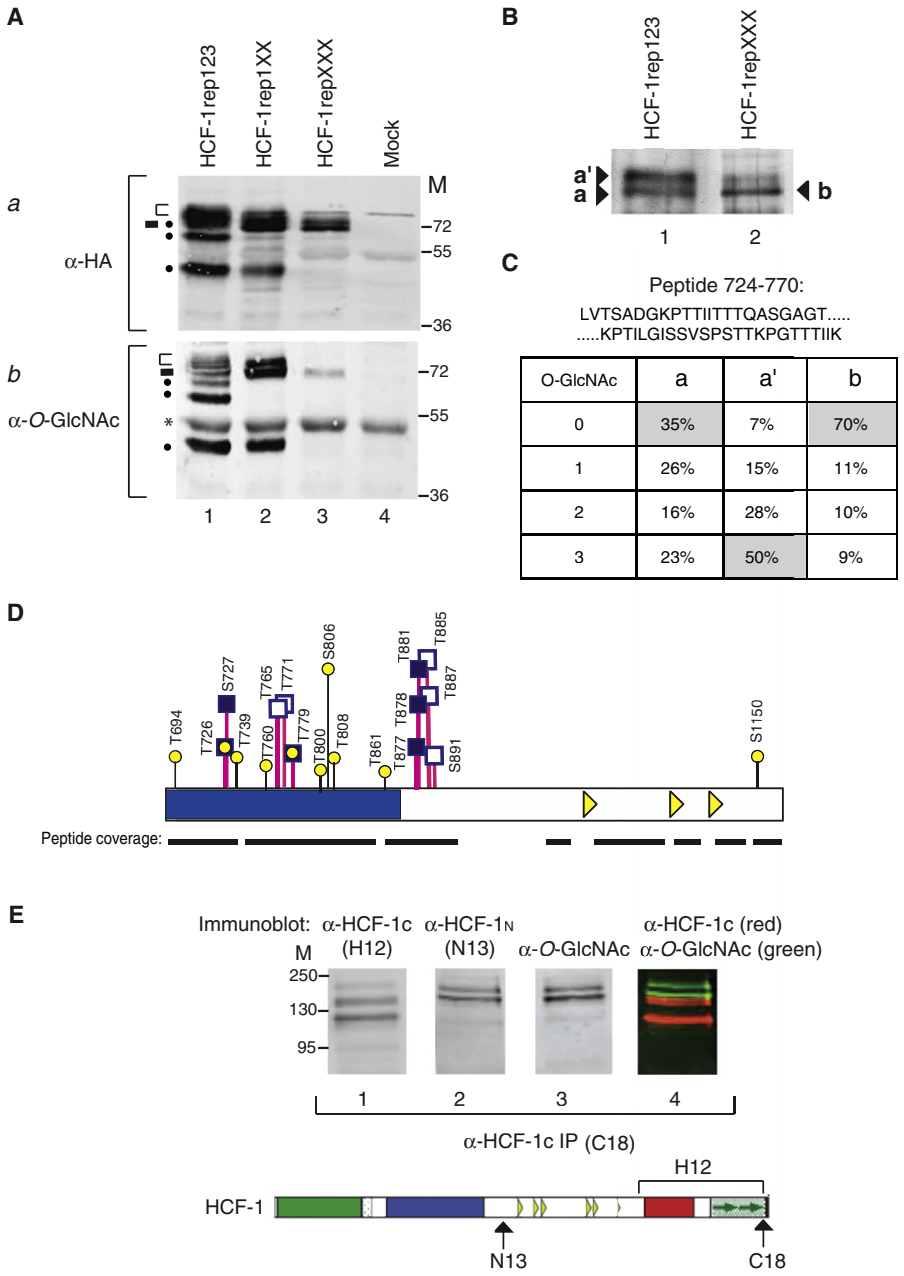

O-GlcNAc	a	a'	b
0	35%	7%	70%
1	26%	15%	11%
2	16%	28%	10%
3	23%	50%	9%

Figure 3. Analysis of HCF-1rep123 *O*-GlcNAcylation

(A) HCF-1_{PRO}-repeat-dependent HCF-1rep123 *O*-GlcNAcylation. 293 cells were mock transfected (lane 4), or transfected with different HCF-1rep123 expression vectors (lanes 1–3; see Figure 2A). α-HA immunoprecipitated proteins were visualized by α-HA tag (panel a) or α-*O*-GlcNAc (panel b) immunoblot. Precursor proteins (–), cleavage products (●), and *O*-GlcNAc-modified proteins (bracket) are indicated. The asterisk indicates an immunoglobulin heavy chain. See also Figure S1.

(B) Purification of HCF-1_{PRO}-repeat precursors. HCF-1rep123 (lane 1) and HCF-1repXXX (lane 2) were synthesized in 293 cells, immunoprecipitated, and visualized by silver staining. Different HCF-1rep123 (a and a′) and HCF-1repXXX (b) forms are indicated.

(C) Relative abundance of peptides corresponding to HCF-1 residues 724–770 with 0, 1, 2, or 3 *O*-GlcNAc moieties attached in samples a, a′, and b from (B) (gray boxes indicate the predominant peptide species for each sample; see Table S1 for the complete list of *O*-GlcNAcylated peptides).

(D) Schematic representation of mapped HCF-1rep123 *O*-GlcNAc sites. HCF-1rep123 regions covered by the MS analysis are indicated below the diagram. Filled and empty squares indicate certain or potential *O*-GlcNAcylation residues, respectively. Yellow dots indicate Wang et al. (2010)-identified *O*-GlcNAcylated residues.

(E) Endogenous HCF-1 *O*-GlcNAcylation. HCF-1 was immunoprecipitated from 293 cells with the C18 α-HCF-1 antibody and visualized by H12 (lane 1), N13 (lane 2), α-*O*-GlcNAc (lane 3), or combined H12 and α-*O*-GlcNAc (lane 4) immunoblot. Regions recognized by the different α-HCF-1 antibodies are indicated below.

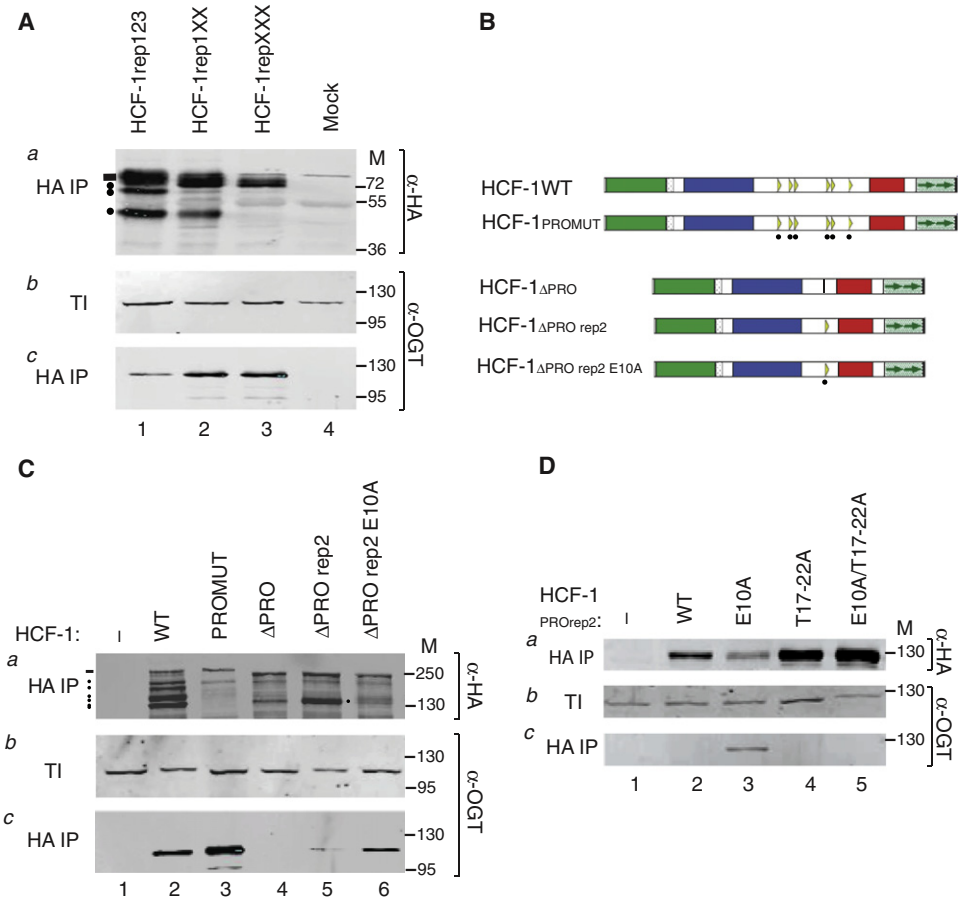

Figure 4. Interaction between OGT and the HCF-1$_{PRO}$ Repeats

(A) OGT coimmunoprecipitation with wild-type and mutant HCF-1$_{PRO}$-repeat constructs. Immunoprecipitated samples from Figure 3A (and reshown in panel a) were probed for OGT coimmunoprecipitation as described below. IP, immunoprecipitate; TI, total input.

(B) Schematic representation of different HCF-1$_{PRO}$-repeat mutants. Dots indicate E10A-mutated HCF-1$_{PRO}$ repeats.

(C) OGT interaction with HCF-1$_{PRO}$-repeat mutants. 293 cells were mock transfected (lane 1) or transfected with the different HCF-1$_{PRO}$-repeat mutant constructs (lanes 2–6). Unlabeled bands represent nonspecific species. In (A) and (C), precursor proteins (–) and cleavage products (●) are indicated.

(D) Effect of mutations in HCF-1$_{PRO}$ repeat 2 on interaction with OGT. 293 cells were mock transfected (lane 1), or transfected with a wild-type (lane 2) or mutated (lanes 3–5) Oct-1/rep2 precursor with the indicated HCF-1$_{PROrep2}$.

In (A), (C), and (D), immunoprecipitated samples were visualized by α-HA tag (panel a) and α-OGT (panel c) immunoblot. Total input (TI) samples visualized by α-OGT immunoblot are shown in panel b.

embedded in the heterologous protein Oct-1 (Oct-1/rep2; Wilson et al., 1995) as shown in Figure 4D. In this assay, wild-type HCF-1$_{PRO}$-repeat 2–OGT interaction was not detectable (lane 2), but the E10A mutation increased OGT association sufficiently to make it clearly detectable (lane 3). In contrast, alanine substitution of four essential threonines (T17, T19, T21, and T22) in the threonine region (T17–22 mutation) did not increase OGT HCF-1$_{PRO}$-repeat binding (lane 4), and indeed inhibited binding when combined as a double mutant with the E10A mutation (compare lanes 3 and 5). Thus, OGT association with the HCF-1$_{PRO}$ repeat is influenced by mutations in both the cleavage and threonine regions.

OGT Cleaves the HCF-1$_{PRO}$ Repeat In Vitro

The aforementioned results suggest that OGT has an intimate role in HCF-1$_{PRO}$-repeat cleavage. To define this role further, we began by testing the ability of recombinant human OGT (rhOGT) purified after synthesis in either insect Sf9 cells (Ins$_{synt}$) or *Escherichia coli* (Bac$_{synt}$) (see Figures S2A and S2B) to induce in vitro cleavage of the HCF-1rep123 precursor in the presence of the OGT cofactor UDP-GlcNAc. As shown in Figure 5A (lanes 1–3), both these rhOGT preparations can cleave the HCF-1rep123 precursor synthesized by in vitro translation in a rabbit reticulocyte lysate (RRL). (The HCF-1rep123 fragment mobility difference in lanes 2 and 3 probably reflects the greater *O*-GlcNAc transferase activity of the Ins$_{synt}$ versus Bac$_{synt}$ rhOGT) (Figure S2C). In the RRL, the HCF-1rep123 precursor is *O*-GlcNAcylated during synthesis (data not shown). To avoid this glycosylation, we synthesized the precursor in a plant wheat germ extract (WGE) which lacks OGT activity (Starr and Hanover, 1990). This precursor was also effectively cleaved by the rhOGT preparations (compare lanes 4–6 and 1–3), showing that

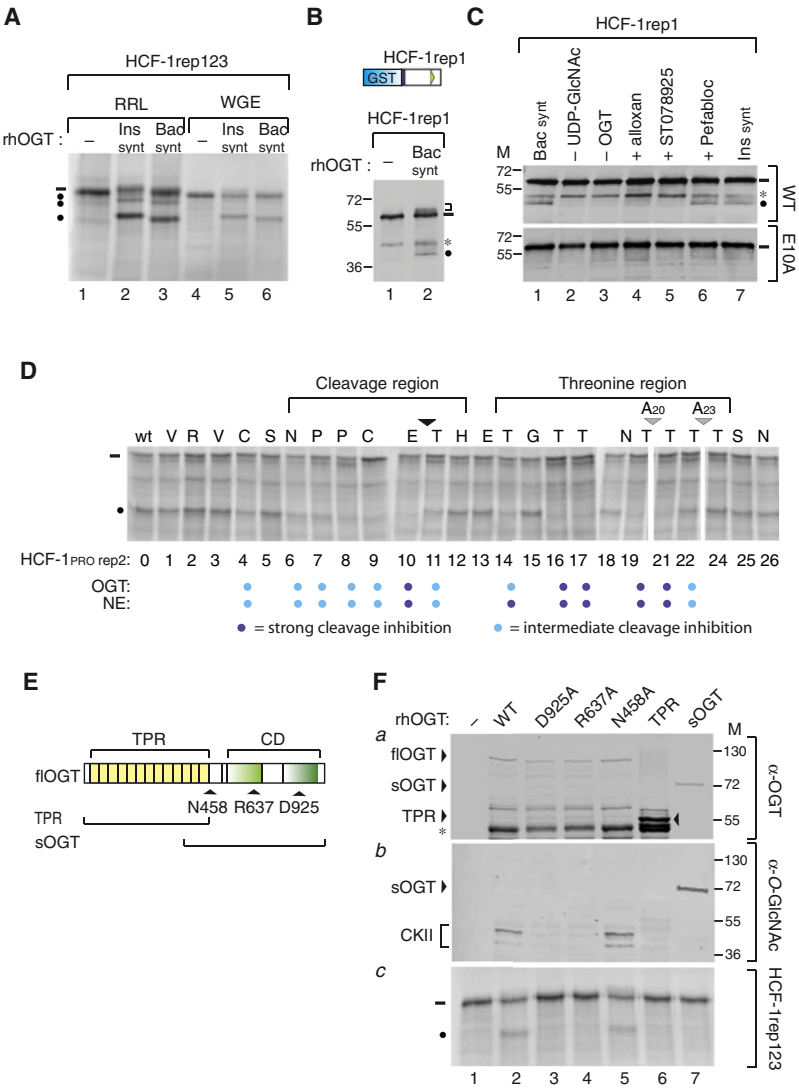

Figure 5. Recombinant OGT Is Sufficient to Induce HCF-1$_{PRO}$-Repeat Cleavage In Vitro

(A) Recombinant human OGT (rhOGT) cleavage of in vitro synthesized HCF-1$_{PRO}$-repeat precursors. The HCF-1rep123 precursor was synthesized in vitro using RRL (lanes 1–3) or WGE (lanes 4–6) and incubated with buffer (lanes 1 and 4), or rhOGT synthesized and purified from insect cells (Ins$_{synt}$; lanes 2 and 5) or from bacterial cells (Bac$_{synt}$; lanes 3 and 6). See also Figures S2A–S2C.

(B) rhOGT cleavage of a bacterially synthesized HCF-1$_{PRO}$-repeat precursor. The GST-HCF-1rep1 precursor (see schematic) synthesized in and purified from bacteria and incubated without (lane 1) or with (lane 2) Bac$_{synt}$ rhOGT. HCF-1$_{PRO}$-repeat 1 cleavage was analyzed by α-GST immunoblot. The asterisk indicates an N-terminal precursor truncation and the bracket indicates the *O*-GlcNAc-modified form of the precursor. See also Figure S2D.

(C) rhOGT HCF-1$_{PRO}$-repeat cleavage characterization. GST-HCF-1rep1 precursors containing wild-type (WT) or E10A-mutated HCF-1$_{PRO}$ repeat 1 were subjected to in vitro cleavage in the presence (+) or absence (–) of the indicated factors. The asterisk indicates an N-terminal precursor truncation.

(D) rhOGT cleavage of HCF-1$_{PRO}$-repeat 2 alanine-scan mutants. The analysis was performed as in Figure 1C using Bac$_{synt}$ rhOGT and WGE synthesized precursors. Dots indicate mutations with strong (blue) and intermediate (cyan) effects on cleavage. The results with HeLa cell nuclear extract (NE) from Figure 1C are shown for reference.

(E) Schematic representation of full-length (flOGT), truncated, and alanine-substitution rhOGT constructs.

(F) The wild-type and indicated OGT mutants were synthesized and purified from *E. coli* and then visualized by α-OGT immunoblot (panel a). The *O*-GlcNAc transferase activity of rhOGT molecules was determined by OGT self-glycosylation and CKII *O*-GlcNAcylation using the α-*O*-GlcNAc antibody (panel b). Proteolytic activity was determined by HCF-1rep123 in vitro cleavage (panel c). The asterisk indicates a nonspecific band.

In (A)–(D) and (F), the precursor proteins (–) and cleavage products (●) are indicated.

precursor *O*-GlcNAcylation prior to the cleavage reaction is not required for HCF-1$_{PRO}$-repeat cleavage.

These results led us to test for HCF-1$_{PRO}$-repeat cleavage by OGT directly. To this end, we used an HCF-1$_{PRO}$-repeat substrate and OGT both synthesized in and purified from bacteria. Owing to the insolubility of the HCF-1rep123 precursor synthesized in bacteria, we designed the smaller HCF-1 precursor illustrated in Figure 5B spanning a single HCF-1$_{PRO}$ repeat 1 (either wild-type or E10A mutant) fused to GST (GST-HCF-1rep1). As shown in Figure 5B, Bac$_{synt}$ OGT cleaved (as well as *O*-GlcNAcylated; Figure S2D) the wild-type GST-HCF-1rep1 precursor, showing that OGT itself induces HCF-1$_{PRO}$-repeat cleavage.

OGT Glycosylation Activity Is Important for HCF-1$_{PRO}$-Repeat Cleavage

To probe the importance of the *O*-GlcNAcylation activity of OGT for HCF-1$_{PRO}$-repeat proteolysis, we determined the dependence of proteolysis on the UDP-GlcNAc cofactor and its sensitivity to an OGT inhibitor. As shown in Figure 5C, both Bac$_{synt}$ (lane 1) and Ins$_{synt}$ (lane 7) OGT were active on the bacterially synthesized wild-type (top), but not E10A point mutant (bottom), HCF-1rep1 precursor, but removal of either UDP-GlcNAc or OGT prevented cleavage (top, lanes 2 and 3). The requirement for two components—OGT and its UDP-GlcNAc cofactor—for HCF-1$_{PRO}$-repeat proteolysis explains the resistance of the HeLa cell HCF-1$_{PRO}$-repeat proteolytic activity to fractionation.

Alloxan, used to inhibit *O*-GlcNAcylation in Figure 2B, is a relatively nonspecific inhibitor that apparently mimics the uracil moiety of the UDP-GlcNAc cofactor (Konrad et al., 2002). Here, to inactivate OGT glycosylation, we additionally used the more specific inhibitor ST078925 (Gross et al., 2005), which also inhibited HCF-1$_{PRO}$-repeat proteolysis (compare lane 1 with lanes 4 and 5). In contrast, as described previously for the HeLa cell activity (Capotosti et al., 2007), OGT-induced

HCF-1_{PRO}-repeat proteolysis is resistant to the serine protease inhibitor Pefabloc (lane 6), showing that it differs from the HCF-1 autocatalytic activity described by Vogel and Kristie (2000).

OGT HCF-1_{PRO}-Repeat Cleavage Is Dependent on the Complete HCF-1_{PRO}-Repeat Signal

In Figure 5D, we show that the Bac_{synt} rhOGT cleavage pattern of the set of 24 HCF-1_{PRO}-repeat 2 alanine-scan mutants synthesized in WGE is essentially the same as that with the HeLa cell nuclear extract (compare with Figure 1C). Thus, OGT itself appears to recognize the large HCF-1_{PRO}-repeat signal and to reproduce entirely the HeLa cell proteolytic activity.

Both the TPR and Catalytic Domains of OGT Are Important for HCF-1_{PRO}-Repeat Proteolysis

To identify elements of OGT required for HCF-1_{PRO}-repeat proteolysis, we assayed the activities of a set of Bac_{synt} rhOGT mutants previously characterized for *O*-GlcNAc transferase activity on either heterologous substrates or for self-glycosylation (Clarke et al., 2008; Gross et al., 2005; Hanover et al., 2003; Martinez-Fleites et al., 2008). As shown in Figure 5E, we analyzed two truncations: one containing the TPR region and one corresponding to an OGT splice variant (sOGT) lacking most of the TPR region (Hanover et al., 2003). We also analyzed three OGT alanine-substitution mutants (Clarke et al., 2008): N458A between the TPR and catalytic domain (CD); R637A in the CD; and D925A in the UDP-GlcNAc binding pocket.

Bac_{synt} wild-type and mutant rhOGT proteins (Figure 5Fa) were tested for their *O*-GlcNAc transferase activity on the heterologous substrate casein kinase II (CKII) as well as by self-glycosylation (Figure 5Fb). Only the wild-type and N458A mutant displayed evident CKII *O*-GlcNAc transferase activity (Figure 5Fb, lanes 2 and 5). Consistent with its reported activities (Hanover et al., 2003; Clarke et al., 2008), the sOGT protein did not exhibit CKII *O*-GlcNAc transferase activity but displayed enhanced self-glycosylation activity (Figures 5Fa and 5Fb, compare lanes 7 and 2), whereas the TPR mutant was inactive.

Among the set of rhOGT mutants, there was a perfect correlation between the ability to *O*-GlcNAcylate the heterologous CKII substrate and to induce HCF-1rep123 proteolysis (Figure 5Fc). In contrast, there was not such a correlation with self-glycosylation activity, as the sOGT form did not display HCF-1rep123 proteolytic activity (Figures 5Fb and 5Fc, lane 7). These results suggest (1) that both the TPR and CD regions of OGT are required for HCF-1_{PRO}-repeat proteolysis and (2) that residues involved in *O*-GlcNAc transferase activity are important for HCF-1_{PRO}-repeat proteolysis.

OGT-Induced *O*-GlcNAcylation Is Not Sufficient to Induce HCF-1_{PRO}-Repeat Proteolysis

Although OGT appears to induce HCF-1_{PRO}-repeat proteolysis on its own, the aforementioned studies do not discriminate between whether (1) OGT *O*-GlcNAcylation of HCF-1 induces HCF-1_{PRO}-repeat autoproteolysis or (2) OGT possesses a previously unrecognized site-specific proteolytic activity that can induce cleavage of the HCF-1_{PRO} repeats either entirely on its own or in collaboration with the HCF-1_{PRO} repeat.

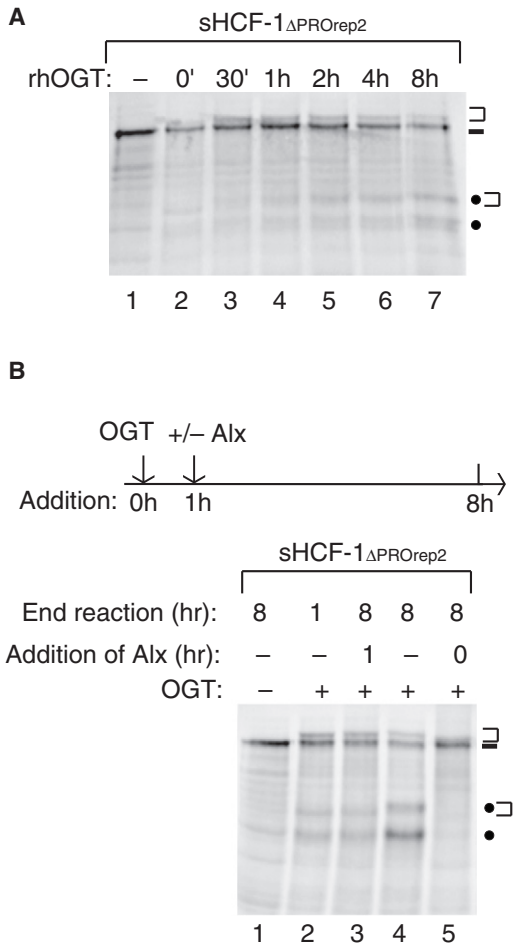

Figure 6. The *O*-GlcNAc Modification of the HCF-1_{PRO}-Repeat Precursor Is Not Sufficient to Induce Proteolysis

(A) Time course of sHCF-$1_{\Delta PROrep2}$ precursor treatment with Bac_{synt} rhOGT.

(B) OGT inhibition during sHCF-$1_{\Delta PROrep2}$ cleavage. The sHCF-$1_{\Delta PROrep2}$ precursor was treated as indicated in the schematic experimental flow chart (top). The sHCF-$1_{\Delta PROrep2}$ precursor synthesized in WGE was incubated with Bac_{synt} rhOGT without (lanes 2 and 4) or with (lanes 3 and 5) addition of alloxan (Alx) and terminated at the times indicated.

Precursor protein (–), both cleavage products (●), and *O*-GlcNAc-modified proteins (brackets) are indicated. See also Figure S3.

To discriminate between these two possibilities, we developed an assay in which glycosylation and proteolysis could be clearly monitored simultaneously. This assay takes advantage of a "short" version, called sHCF-$1_{\Delta PROrep2}$, of the HCF-$1_{\Delta PROrep2}$ precursor shown in Figure 4B; it exhibits a clear electrophoretic mobility shift upon *O*-GlcNAcylation (see Figure S3). As shown in Figure 6A, with this precursor, within a 30 min incubation with the Bac_{synt} rhOGT (lane 3), a retarded *O*-GlcNAcylated form is apparent (indicated by the bracket). This *O*-GlcNAc-modified precursor increased for up to 2 hr and then slowly disappeared as two cleavage products accumulated—a slower-migrating N-terminal and faster-migrating C-terminal cleavage product (indicated by dots). We used the clear appearance of both *O*-GlcNAcylated precursor and

cleavage products to probe the direct or indirect role of OGT in HCF-1_{PRO}-repeat proteolysis.

We used alloxan to block OGT activity at different time points and then examined the effects on HCF-1_{PRO}-repeat proteolysis. We initiated a series of sHCF-$1_{\Delta PROrep2}$ cleavage reactions by addition of OGT (see Figure 6B, top). OGT was then inactivated by addition of alloxan at either the start of the reaction (0 hr), which prevented its function throughout the experiment (lane 5), or after 1 hr, at which point there was initial sHCF-$1_{\Delta PROrep2}$ precursor *O*-GlcNAcylation but little cleavage (lane 3). Two control reactions were terminated at 1 hr (lane 2) or 8 hr (lane 4) without the addition of alloxan. These control reactions showed that, after 1 hr, the *O*-GlcNAcylated precursor and some cleavage products appeared (compare lanes 2 and 1) and, after 8 hr, the cleavage products became more abundant whereas the *O*-GlcNAcylated precursor did not (lane 4). Addition of alloxan after 1 hr (lane 3) resulted in arresting the reaction such that after 8 hr the *O*-GlcNAcylation and cleavage pattern were essentially identical to that after 1 hr (compare lanes 2–4). Thus, there is no apparent cleavage of the *O*-GlcNAcylated sHCF-$1_{\Delta PROrep2}$ precursor in the absence of OGT function. These results suggest that the *O*-GlcNAcylated HCF-1 precursor is not potentiated for independent autoproteolysis. We conclude that OGT possesses a proteolytic activity which may be wholly contained within OGT or function in intimate collaboration with the HCF-1_{PRO} repeat (see Discussion).

A Heterologous Protease Cleavage Site Fails to Restore HCF-1_C-Subunit Function

Given the evident unusual nature of HCF-1 proteolytic maturation, we asked whether this specific process is important for the HCF-1_C-subunit function in M phase (see Introduction). For this, we replaced the HCF-1_{PRO}-repeat region with the two natural Taspase1 protease cleavage sites found in MLL (Hsieh et al., 2003) to create HCF-$1_{\Delta PROMLL}$ (see Figure 7A). Given that Taspase1 naturally cleaves the *Drosophila* HCF-1 homolog, this experiment addresses whether the appearance of HCF-1_{PRO}-repeat-induced HCF-1 maturation was evolutionarily significant.

We first tested for OGT interaction with the HCF-$1_{\Delta PROMLL}$ mutant. As shown in Figure 7B, HCF-$1_{\Delta PROMLL}$ is effectively cleaved in 293 cells (Figure 7Ba, lane 4) but, like HCF-$1_{\Delta PRO}$, is defective for OGT binding (Figure 7Bc, lanes 2–4). Thus, replacement of the HCF-1_{PRO} repeats with the MLL Taspase1 cleavage sites separates HCF-1 proteolysis from evident OGT binding.

We then asked whether the HCF-$1_{\Delta PROMLL}$ protein is able to rescue the M phase binucleation defect induced by loss of HCF-1 processing (Julien and Herr, 2003). We produced a cell line expressing an siRNA-resistant HCF-$1_{\Delta PROMLL}$ protein, selectively depleted the endogenous HCF-1 protein by siRNA, and counted the number of binucleated cells. As shown in Figure 7C, only the wild-type full-length HCF-1 (WT) and to a lesser extent the HCF-1_C subunit (C600) but not the HCF-$1_{\Delta PRO}$ protein were able to rescue the binucleation phenotype induced by the lost of endogenous HCF-1. (The inability of the HCF-$1_{\Delta PRO}$ protein to rescue the binucleation phenotype is not owing to the absence of the HCF-1_{PRO}-repeat region per se because the HCF-1_{PROMUT} protein shown in Figure 4B also displays binucleation defects; S.G. and W.H., unpublished results.) Interestingly, the cleaved HCF-$1_{\Delta PROMLL}$ protein is not able to rescue the binucleation defect, suggesting that HCF-1_{PRO}-repeat-mediated HCF-1 proteolytic maturation—and probably HCF-1_N *O*-GlcNAcylation—are important to activate the M phase functions of the HCF-1_C subunit.

DISCUSSION

We have investigated the mechanisms of HCF-1 proteolytic maturation and identified a link between OGT-induced HCF-1 proteolysis and *O*-GlcNAcylation. OGT binds and cleaves the HCF-1_{PRO} repeats while inducing *O*-GlcNAcylation of the HCF-1_N subunit. This link is associated with activation of the M phase regulatory functions of HCF-1. These activities of OGT connect the class of reversible posttranslational modifications such as glycosylation with essentially irreversible proteolytic processing.

How we arrived at these conclusions was circuitous. We began by hypothesizing that HCF-1_{PRO}-repeat cleavage involves modification of a series of highly conserved and important threonines. Indeed, modification—*O*-GlcNAcylation—is important, but the HCF-1_{PRO} repeat is apparently not the target of this modification. Instead, it is the binding site for OGT, which then promotes *O*-GlcNAcylation elsewhere as well as cleavage of its own binding site.

A Bipartite Association of OGT with the HCF-1_{PRO} Repeat

The analysis of OGT binding to the HCF-1_{PRO} repeat suggests that it recognizes both the cleavage and threonine regions: thus, OGT displays enhanced association with a cleavage-region mutant (E10A), and a threonine-region mutant (T17–22A) counteracts this enhancement (see Figure 4). The inhibition of OGT association by the threonine-region mutant suggests that OGT does not recognize and bind the cleavage region effectively on its own. We suggest that the threonine region represents a site for stable OGT interaction. The enhanced association of OGT with the E10A mutant was not expected. Given that the E10 residue is immediately adjacent to the cleavage site, we suggest that this residue associates with the catalytic center of OGT. If OGT association with the HCF-1_{PRO} repeat is reduced upon proteolytic cleavage, then inhibition of cleavage by the E10A mutation could enhance OGT binding to the HCF-1_{PRO} repeat by retaining OGT on the noncleavable site. Thus, OGT is essentially "trapped" on the E10A mutant.

We find intriguing the bipartite TPR and CD structure of OGT and the bipartite threonine and cleavage structure of the HCF-1_{PRO} repeat. We suggest a one-to-one correspondence between the OGT TPR region and HCF-1_{PRO}-repeat threonine region for binding and OGT CD region and HCF-1_{PRO}-repeat cleavage region for HCF-1_{PRO}-repeat proteolysis. This hypothesis can explain the surprisingly large sequence required for HCF-1_{PRO}-repeat-induced proteolysis.

Although we initiated our studies hypothesizing that the threonine region would serve as a site for modification to activate HCF-1_{PRO}-repeat proteolysis, we now imagine that the inverse might be true: *O*-GlcNAcylation of the threonine region inhibits OGT binding to the HCF-1_{PRO} repeat, which could be used to inhibit HCF-1 proteolytic maturation.

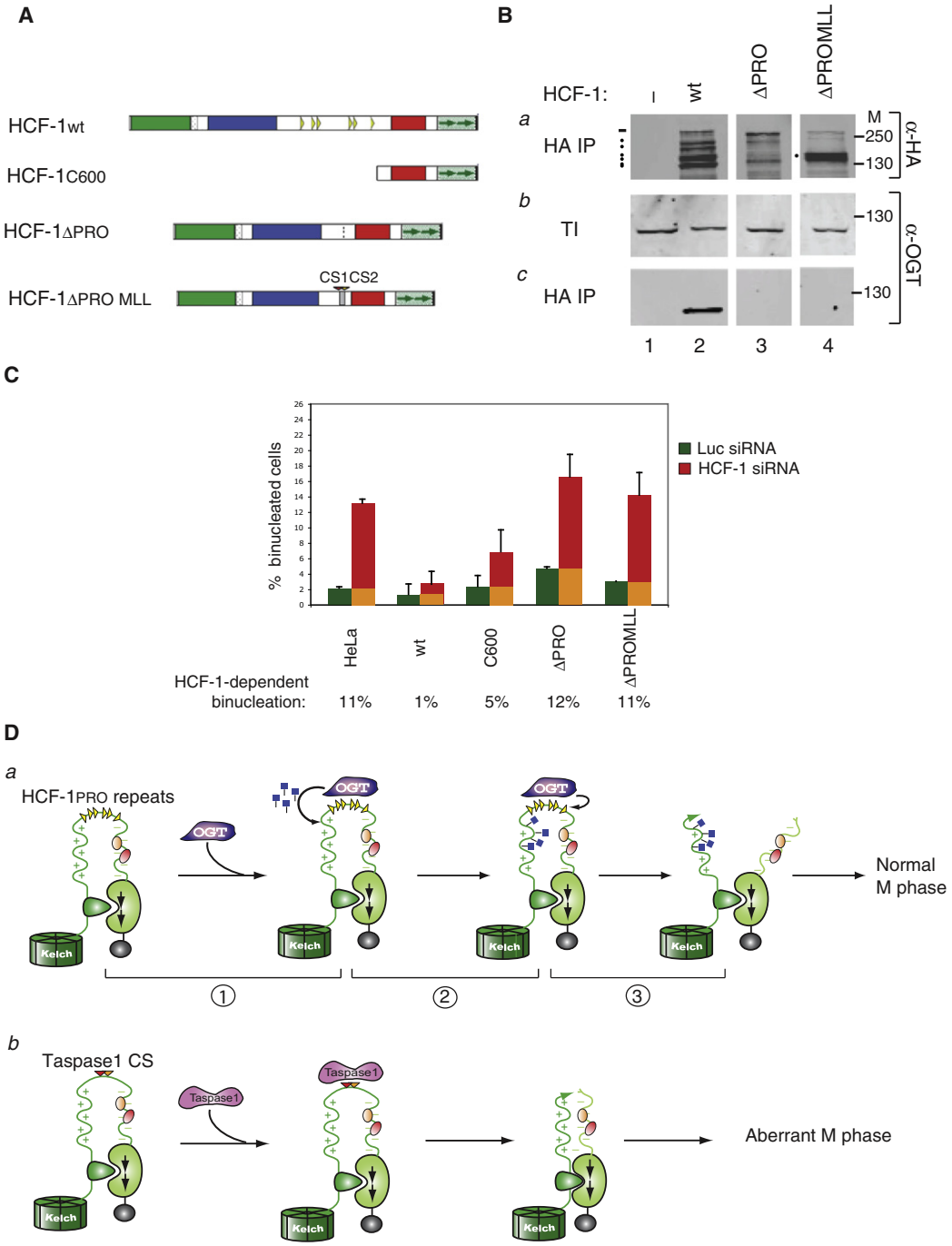

Figure 7. OGT-Mediated HCF-1$_{PRO}$-Repeat Proteolysis Is Important for HCF-1$_C$ Function

(A) Schematic representation of different HCF-1 recombinants. CS1 and CS2 indicate the two Taspase1 cleavage sites of the MLL protein (Hsieh et al., 2003).

(B) OGT association assay with HCF-1 protein carrying the MLL Taspase1 sites. Lanes 1–3 are as shown in Figure 4C. Lane 4: 293 cells transfected with the HCF-1$_{\Delta PROMLL}$ construct. Immunoprecipitated samples were visualized by α-HA tag (panel a) and α-OGT (panel c) immunoblot. Total input (TI) samples were visualized by α-OGT immunoblot (panel b). Precursor proteins (–) and cleavage products (●) are indicated.

(C) Quantification of binucleated cells in the parental Flp-In-HeLa cells as well as in the indicated cell lines after control (Luc; green) or HCF-1 (red/orange) siRNA (data are represented as mean ± SD). In orange is indicated the background level of binucleation for each sample. The percentages below the histogram indicate differences between the Luc and HCF-1 siRNA for each sample.

(D) Proposed model for OGT-induced HCF-1$_{PRO}$-repeat proteolytic maturation showing potential consequences for HCF-1-protein conformation and function (see text). Kelch indicates an N-terminal Kelch-repeat domain.

OGT: An Unusual Protease

The large sequence required for HCF-1_{PRO}-repeat-induced proteolysis had suggested that the HCF-1_{PRO} repeat would be cleaved by an unusual mechanism. The discovery that OGT is responsible for HCF-1_{PRO}-repeat cleavage is consistent with this hypothesis.

We imagine two principal ways in which OGT might cleave the HCF-1_{PRO} repeat: OGT could possess a catalytic center for proteolysis or function as a coprotease to cleave HCF-1 in collaboration with the HCF-1_{PRO} repeat. Relative to the first hypothesis, we have not been able to identify a protease-like domain. Nevertheless, OGT is distantly related to enzymes that, like proteases, are hydrolases (Wrabl and Grishin, 2001), and thus OGT might possess an unusual proteolytic catalytic center.

In the second preferred hypothesis, OGT functions in intimate collaboration with the HCF-1_{PRO} repeat for cleavage. For example, OGT might stimulate HCF-1_{PRO}-repeat cleavage similarly to *E. coli* RecA-induced autocleavage of the LexA repressor (Luo et al., 2001). Here, RecA binding to LexA induces a conformational change of LexA, allowing for a repositioning of the LexA active and cleavage sites for autocleavage. By analogy, OGT binding to the HCF-1_{PRO} repeat might lead to a change in conformation that stimulates hydrolysis, for example by activating the essential E10 residue at the cleavage site. We also imagine that GlcNAc moieties on HCF-1 could in turn play a specific role in cleavage. For example, GlcNAc could be bound by—or remain bound to—OGT via its UDP-GlcNAc pocket and, as such, either directly (e.g., participate in catalysis) or indirectly (e.g., play a conformational role) stimulate HCF-1_{PRO}-repeat cleavage. Such a mechanism could ensure coordinate HCF-1 *O*-GlcNAcylation and cleavage.

A Proteolytic Cleavage Signal Regulates Posttranslational Modification: A Model for HCF-1 Maturation

Proteolytic maturation of HCF-1 was known to be important for the biological functions of HCF-1. It is now evident that HCF-1 proteolytic maturation involves not only proteolysis but also *O*-GlcNAc modification, and that the interplay between these two modifications is what appears to regulate HCF-1 function in M phase. We propose in Figure 7Da a three-step mechanism for HCF-1 maturation: OGT (1) associates with the elaborate HCF-1_{PRO}-repeat signal, (2) *O*-GlcNAcylates the HCF-1_N subunit, and (3) cleaves the protein. In contrast, we suggest that Taspase1-induced HCF-1 cleavage circumvents the *O*-GlcNAcylation step (Figure 7Db) and that this step is critical for activation of the HCF-1_C subunit for M phase progression. The HCF-1_N basic and HCF-1_C acidic regions are known to associate noncovalently with one another (Wilson et al., 2000). Perhaps repeated *O*-GlcNAc modification within and around the HCF-1_N basic region induced by the presence of multiple HCF-1_{PRO} repeats disrupts this HCF-1_N and HCF-1_C interaction, functionally liberating transcriptional activation (in orange; Luciano and Wilson, 2002) and chromatin association (in red; Julien and Herr, 2004) domains present in the HCF-1_C acidic region.

Why Involve OGT in HCF-1 Maturation?

OGT has been hypothesized to serve as a sensor for the metabolic state of the cell by responding to glucose levels (Butkinaree et al., 2010; Love et al., 2010). Because HCF-1 promotes cell proliferation and cell proliferation is associated with enhanced nutrient supplies that generate glucose, we suggest that a role for OGT in activation of HCF-1 via proteolytic maturation involving *O*-GlcNAcylation can link the cellular activities of HCF-1 to the metabolic state of the cell.

EXPERIMENTAL PROCEDURES

Plasmid Constructs and DNA Template Preparation

Plasmids and DNA templates are described in Extended Experimental Procedures.

Cell Culture, Extract Preparation, and Plasmid and siRNA Transfections

Human HeLa and 293 cells were grown on plates at 37°C in DMEM with 10% FBS. Nuclear extracts for in vitro cleavage assay were prepared from spinner HeLa cells as previously described (Dignam et al., 1983). Plasmid and siRNA transfections were performed with Lipofectamine or Oligofectamine, respectively, as described (Invitrogen) (see also Extended Experimental Procedures).

Synthesis and Purification of Recombinant Proteins from Bacterial and Insect Cells

For GST–HCF-1rep1WT and GST–HCF-1rep1E10A synthesis in *E. coli*, BL21 (DE5) cells were grown at 22°C until an OD_{600} of 0.6 before induction with 0.4 mM IPTG for 4 hr. Cells were lysed with PBS supplemented with lysozyme, and lysates were centrifuged at 13,000 × g for 30 min. SDS was added to a final concentration of 1% and lysates were boiled for 10 min. SDS was then diluted to 0.1% with PBS and the lysates were incubated with Ni beads overnight at 4°C. Proteins were eluted with 500 mM imidazole and dialyzed against PBS. Wild-type and mutant S-tagged human OGTs were synthesized in *E. coli* BL21(DE5) cells. Cells were grown at 25°C until an OD_{600} of 0.6, at which point OGT synthesis was induced with 0.4 mM IPTG and cells were incubated at 16°C for 16 hr. The OGT proteins were purified using the S-tag purification system, as recommended (Novagen). Wild-type Flag-tagged OGT was synthesized in insect Sf9 cells, lysates were prepared, and proteins were immunoprecipitated using immobilized α-Flag magnetic beads (Sigma) and eluted using 0.2 mg/ml of 1× Flag peptide as described (Cai et al., 2006, 2010).

In Vitro Cleavage and *O*-GlcNAc Transferase Assays

In vitro HCF-1_{PRO}-repeat cleavage was performed in 100 mM HEPES (pH 7.9), 5 mM $MgCl_2$, 20 mM KCl, 5 mM DTT, and 10% sucrose at a final volume of 30 μl at 37°C for 16 hr or as specified (Capotosti et al., 2007; Hsieh et al., 2003). For the rhOGT in vitro cleavage assay, 1.5 μg of Ins_{synt} or Bac_{synt} rhOGT preparation was used and the cleavage buffer was supplemented with 5 μM UDP-GlcNAc. The presence of DTT was critical for OGT-induced HCF-1_{PRO}-repeat cleavage. Bacterially purified GST-HCF-1rep1 in vitro cleavage was performed with 500 ng precursor protein. For inhibitor treatment, reactions prior to precursor addition were treated for 30 min at RT with either 2.5 mM alloxan (Konrad et al., 2002), 15 μM staurosporine (Gani and Engh, 2010), 0.5 mg/ml Pefabloc (Vogel and Kristie, 2000), or 500 μM ST078925. The ST078925 inhibitor (4-[(3-cyano-4-(2-thienyl)-2-5,6,7,8-tetrahydroquinolylthio)methyl] benzoic acid; TimTec) is an analog substitute of the validated inhibitor 6 from Gross et al. (2005). For phosphatase treatment, in vitro cleaved HCF-1repXX3 precursor was incubated for 2 hr at 37°C with 400 U of λ phosphatase (PPase) in the absence or presence of 50 mM EDTA. The *O*-GlcNAc transferase assay was performed as described (Clarke et al., 2008) using 2500 U of the CKII substrate.

Nondenaturating Immunoprecipitation

For α-HA tag immunoprecipitation, cells were lysed in 0.5% NP40, 10 mM TrisCl (pH 8.0), 150 mM NaCl, 5 mM $MgCl_2$ (NP40 buffer; Misaghi et al.,

2009). Lysates were incubated with α-HA agarose beads (Sigma) overnight at 4°C, beads were washed extensively in NP40 buffer, and immunoprecipitated material was eluted in SDS-PAGE loading buffer. For endogenous HCF-1 immunoprecipitation, 1.5 mg of 420 mM KCl HeLa nuclear extract was diluted to 100 mM KCl and incubated overnight at 4°C with 10 μl of C18 α-HCF-1_C antibody or 10 μl of nonimmune sera. Samples were analyzed by immunoblot. See Extended Experimental Procedures for the origin of antibodies used and procedure for immunoblot analysis.

O-GlcNAcylation Analysis by LC-MS/MS

HA-tagged HCF-1rep123 plasmid expression vectors were transfected into ten 15 cm dishes of 293 cells for 48 hr. Cells were lysed in 8 ml NP40 buffer. The lysates were adjusted to 1% SDS and boiled for 10 min. The SDS concentration was subsequently adjusted to 0.1% by dilution with NP40 buffer, and lysates were incubated with α-HA agarose beads overnight at 4°C. For proteomic analysis, see Extended Experimental Procedures.

Generation of Cell Lines and Binucleation Analysis

To create the recombinant HCF-1 Flp-In-HeLa cells, 0.4 μg of pCDNA5/HA-FLAG/FRT vector containing genes of interest was cotransfected with 3.6 μg of the Flpase expression vector pOG44 into Flp-In-HeLa cells (a kind gift of S.S. Taylor) with Lipofectamine, and transfected cells were selected in hygromycin-containing medium (300 μg/ml) for 10 days as described (Invitrogen). Three independent clones for each recombinant HCF-1 construct were selected for analysis. Endogenous HCF-1 was depleted by double siRNA treatment for 50 hr and binucleated cells were quantitated by staining with α-tubulin and α-HCF-1_C H12—to determine HCF-1 depletion—antibodies and DAPI as previously described (Julien and Herr, 2003). One hundred cells were counted per siRNA depletion and each independent clone was analyzed in triplicate. Data were summarized as mean ± standard deviation (SD).

SUPPLEMENTAL INFORMATION

Supplemental Information includes Extended Experimental Procedures, three figures, and one table and can be found with this article online at doi:10.1016/j.cell.2010.12.030.

ACKNOWLEDGMENTS

We thank T.M. Kristie and J.A. Hanover for the HCF-1nc and the bacterial OGT expression vectors, respectively; M. Boutros and A. Wilson for the HCF-$1_{\Delta PROrep2}$ construct; R.S. Haltiwanger for the α-OGT antibody; E. Julien and D.J. Aufiero for the N13 and C18 antibodies; S.S. Taylor for the Flp-In-HeLa cells; M. Quadroni for advice with the mass spectrometry analysis; L. Capponi, P. L'Hôte, and M. McLaird for technical support; and J.H. Reina for art design. We thank N. Hernandez, J. Michaud, and S.H. Verhelst for critical reading of the manuscript; and V. Zoete, O. Michielin, N. Hernandez, J. Müller, P. Schneider, and K. Struhl for discussion. This study was supported by the Stowers Institute for Medical Research and the Helen Nelson Medical Research Fund at the Greater Kansas City Community Foundation to J.W.C. and R.C.C. and by the Swiss National Science Foundation, Oncosuisse, and the University of Lausanne to W.H.

Received: August 20, 2010
Revised: November 22, 2010
Accepted: December 16, 2010
Published: February 3, 2011

REFERENCES

Butkinaree, C., Park, K., and Hart, G.W. (2010). O-linked β-N-acetylglucosamine (O-GlcNAc): extensive crosstalk with phosphorylation to regulate signaling and transcription in response to nutrients and stress. Biochim. Biophys. Acta *1800*, 96–106.

Cai, Y., Jin, J., Gottschalk, A.J., Yao, T., Conaway, J.W., and Conaway, R.C. (2006). Purification and assay of the human INO80 and SRCAP chromatin remodeling complexes. Methods *40*, 312–317.

Cai, Y., Jin, J., Swanson, S.K., Cole, M.D., Choi, S.H., Florens, L., Washburn, M.P., Conaway, J.W., and Conaway, R.C. (2010). Subunit composition and substrate specificity of a MOF-containing histone acetyltransferase distinct from the male-specific lethal (MSL) complex. J. Biol. Chem. *285*, 4268–4272.

Capotosti, F., Hsieh, J.J., and Herr, W. (2007). Species selectivity of mixed-lineage leukemia/trithorax and HCF proteolytic maturation pathways. Mol. Cell. Biol. *27*, 7063–7072.

Clarke, A.J., Hurtado-Guerrero, R., Pathak, S., Schuttelkopf, A.W., Borodkin, V., Shepherd, S.M., Ibrahim, A.F., and van Aalten, D.M. (2008). Structural insights into mechanism and specificity of O-GlcNAc transferase. EMBO J. *27*, 2780–2788.

Crooks, G.E., Hon, G., Chandonia, J.M., and Brenner, S.E. (2004). WebLogo: a sequence logo generator. Genome Res. *14*, 1188–1190.

Dignam, J.D., Lebovitz, R.M., and Roeder, R.G. (1983). Accurate transcription initiation by RNA polymerase II in a soluble extract from isolated mammalian nuclei. Nucleic Acids Res. *11*, 1475–1489.

Gani, O.A., and Engh, R.A. (2010). Protein kinase inhibition of clinically important staurosporine analogues. Nat. Prod. Rep. *27*, 489–498.

Goto, H., Motomura, S., Wilson, A.C., Freiman, R.N., Nakabeppu, Y., Fukushima, K., Fujishima, M., Herr, W., and Nishimoto, T. (1997). A single-point mutation in HCF causes temperature-sensitive cell-cycle arrest and disrupts VP16 function. Genes Dev. *11*, 726–737.

Gross, B.J., Kraybill, B.C., and Walker, S. (2005). Discovery of O-GlcNAc transferase inhibitors. J. Am. Chem. Soc. *127*, 14588–14589.

Haltiwanger, R.S., Blomberg, M.A., and Hart, G.W. (1992). Glycosylation of nuclear and cytoplasmic proteins. Purification and characterization of a uridine diphospho-N-acetylglucosamine:polypeptide β-N-acetylglucosaminyltransferase. J. Biol. Chem. *267*, 9005–9013.

Hanover, J.A., Yu, S., Lubas, W.B., Shin, S.H., Ragano-Caracciola, M., Kochran, J., and Love, D.C. (2003). Mitochondrial and nucleocytoplasmic isoforms of O-linked GlcNAc transferase encoded by a single mammalian gene. Arch. Biochem. Biophys. *409*, 287–297.

Hart, G.W., Housley, M.P., and Slawson, C. (2007). Cycling of O-linked β-N-acetylglucosamine on nucleocytoplasmic proteins. Nature *446*, 1017–1022.

Hsieh, J.J., Cheng, E.H., and Korsmeyer, S.J. (2003). Taspase1: a threonine aspartase required for cleavage of MLL and proper HOX gene expression. Cell *115*, 293–303.

Jinek, M., Rehwinkel, J., Lazarus, B.D., Izaurralde, E., Hanover, J.A., and Conti, E. (2004). The superhelical TPR-repeat domain of O-linked GlcNAc transferase exhibits structural similarities to importin α. Nat. Struct. Mol. Biol. *11*, 1001–1007.

Julien, E., and Herr, W. (2003). Proteolytic processing is necessary to separate and ensure proper cell growth and cytokinesis functions of HCF-1. EMBO J. *22*, 2360–2369.

Julien, E., and Herr, W. (2004). A switch in mitotic histone H4 lysine 20 methylation status is linked to M phase defects upon loss of HCF-1. Mol. Cell *14*, 713–725.

Konrad, R.J., Zhang, F., Hale, J.E., Knierman, M.D., Becker, G.W., and Kudlow, J.E. (2002). Alloxan is an inhibitor of the enzyme O-linked N-acetylglucosamine transferase. Biochem. Biophys. Res. Commun. *293*, 207–212.

Kreppel, L.K., and Hart, G.W. (1999). Regulation of a cytosolic and nuclear O-GlcNAc transferase. Role of the tetratricopeptide repeats. J. Biol. Chem. *274*, 32015–32022.

Kristie, T.M., Pomerantz, J.L., Twomey, T.C., Parent, S.A., and Sharp, P.A. (1995). The cellular C1 factor of the herpes simplex virus enhancer complex is a family of polypeptides. J. Biol. Chem. *270*, 4387–4394.

Kristie, T.M., Liang, Y., and Vogel, J.L. (2010). Control of α-herpesvirus IE gene expression by HCF-1 coupled chromatin modification activities. Biochim. Biophys. Acta *1799*, 257–265.

Lazarus, B.D., Love, D.C., and Hanover, J.A. (2006). Recombinant O-GlcNAc transferase isoforms: identification of O-GlcNAcase, yes tyrosine kinase, and tau as isoform-specific substrates. Glycobiology *16*, 415–421.

Love, D.C., Krause, M.W., and Hanover, J.A. (2010). O-GlcNAc cycling: emerging roles in development and epigenetics. Semin. Cell Dev. Biol. *21*, 646–654.

Lubas, W.A., and Hanover, J.A. (2000). Functional expression of O-linked GlcNAc transferase. Domain structure and substrate specificity. J. Biol. Chem. *275*, 10983–10988.

Luciano, R.L., and Wilson, A.C. (2002). An activation domain in the C-terminal subunit of HCF-1 is important for transactivation by VP16 and LZIP. Proc. Natl. Acad. Sci. USA *99*, 13403–13408.

Luo, Y., Pfuetzner, R.A., Mosimann, S., Paetzel, M., Frey, E.A., Cherney, M., Kim, B., Little, J.W., and Strynadka, N.C. (2001). Crystal structure of LexA: a conformational switch for regulation of self-cleavage. Cell *106*, 585–594.

Martinez-Fleites, C., Macauley, M.S., He, Y., Shen, D.L., Vocadlo, D.J., and Davies, G.J. (2008). Structure of an O-GlcNAc transferase homolog provides insight into intracellular glycosylation. Nat. Struct. Mol. Biol. *15*, 764–765.

Mazars, R., Gonzalez-de-Peredo, A., Cayrol, C., Lavigne, A.C., Vogel, J.L., Ortega, N., Lacroix, C., Gautier, V., Huet, G., Ray, A., et al. (2010). The THAP-zinc finger protein THAP1 associates with coactivator HCF-1 and O-GlcNAc transferase: a link between DYT6 and DYT3 dystonias. J. Biol. Chem. *285*, 13364–13371.

Misaghi, S., Ottosen, S., Izrael-Tomasevic, A., Arnott, D., Lamkanfi, M., Lee, J., Liu, J., O'Rourke, K., Dixit, V.M., and Wilson, A.C. (2009). Association of C-terminal ubiquitin hydrolase BRCA1-associated protein 1 with cell cycle regulator host cell factor 1. Mol. Cell. Biol. *29*, 2181–2192.

Nalivaeva, N.N., and Turner, A.J. (2001). Post-translational modifications of proteins: acetylcholinesterase as a model system. Proteomics *1*, 735–747.

Starr, C.M., and Hanover, J.A. (1990). Glycosylation of nuclear pore protein p62. Reticulocyte lysate catalyzes O-linked N-acetylglucosamine addition in vitro. J. Biol. Chem. *265*, 6868–6873.

Torres, C.R., and Hart, G.W. (1984). Topography and polypeptide distribution of terminal N-acetylglucosamine residues on the surfaces of intact lymphocytes. Evidence for O-linked GlcNAc. J. Biol. Chem. *259*, 3308–3317.

Tyagi, S., and Herr, W. (2009). E2F1 mediates DNA damage and apoptosis through HCF-1 and the MLL family of histone methyltransferases. EMBO J. *28*, 3185–3195.

Vogel, J.L., and Kristie, T.M. (2000). Autocatalytic proteolysis of the transcription factor-coactivator C1 (HCF): a potential role for proteolytic regulation of coactivator function. Proc. Natl. Acad. Sci. USA *97*, 9425–9430.

Vogel, J.L., and Kristie, T.M. (2006). Site-specific proteolysis of the transcriptional coactivator HCF-1 can regulate its interaction with protein cofactors. Proc. Natl. Acad. Sci. USA *103*, 6817–6822.

Wang, Z., Udeshi, N.D., Slawson, C., Compton, P.D., Sakabe, K., Cheung, W.D., Shabanowitz, J., Hunt, D.F., and Hart, G.W. (2010). Extensive crosstalk between O-GlcNAcylation and phosphorylation regulates cytokinesis. Sci. Signal. *3*, ra2.

Wells, L., and Hart, G.W. (2003). O-GlcNAc turns twenty: functional implications for post-translational modification of nuclear and cytosolic proteins with a sugar. FEBS Lett. *546*, 154–158.

Wells, L., Vosseller, K., and Hart, G.W. (2001). Glycosylation of nucleocytoplasmic proteins: signal transduction and O-GlcNAc. Science *291*, 2376–2378.

Wells, L., Kreppel, L.K., Comer, F.I., Wadzinski, B.E., and Hart, G.W. (2004). O-GlcNAc transferase is in a functional complex with protein phosphatase 1 catalytic subunits. J. Biol. Chem. *279*, 38466–38470.

Wilson, A.C., LaMarco, K., Peterson, M.G., and Herr, W. (1993). The VP16 accessory protein HCF is a family of polypeptides processed from a large precursor protein. Cell *74*, 115–125.

Wilson, A.C., Peterson, M.G., and Herr, W. (1995). The HCF repeat is an unusual proteolytic cleavage signal. Genes Dev. *9*, 2445–2458.

Wilson, A.C., Boutros, M., Johnson, K.M., and Herr, W. (2000). HCF-1 amino- and carboxy-terminal subunit association through two separate sets of interaction modules: involvement of fibronectin type 3 repeats. Mol. Cell. Biol. *20*, 6721–6730.

Wrabl, J.O., and Grishin, N.V. (2001). Homology between O-linked GlcNAc transferases and proteins of the glycogen phosphorylase superfamily. J. Mol. Biol. *314*, 365–374.

Wysocka, J., and Herr, W. (2003). The herpes simplex virus VP16-induced complex: the makings of a regulatory switch. Trends Biochem. Sci. *28*, 294–304.

Wysocka, J., Myers, M.P., Laherty, C.D., Eisenman, R.N., and Herr, W. (2003). Human Sin3 deacetylase and trithorax-related Set1/Ash2 histone H3-K4 methyltransferase are tethered together selectively by the cell-proliferation factor HCF-1. Genes Dev. *17*, 896–911.

Yang, X., Zhang, F., and Kudlow, J.E. (2002). Recruitment of O-GlcNAc transferase to promoters by corepressor mSin3A: coupling protein O-GlcNAcylation to transcriptional repression. Cell *110*, 69–80.